Original Article

Quantitative analysis of ^{68}Ga-DOTA(0)-Tyr(3)-octreotate positron emission tomography/computed tomography imaging for the differential diagnosis of primary pheochromocytoma and paraganglioma

Guangyu Ma[1#], Jin Du[2#], Xiaojun Zhang[1], Jiajin Liu[1], Xiaodan Xu[1], Baixuan Xu[1], Zhiwei Guan[1,3]

[1]Department of Nuclear Medicine, Chinese PLA General Hospital, Beijing, China; [2]Department of Endocrinology, Chinese PLA General Hospital, Beijing, China; [3]National Clinical Research Center for Geriatric Diseases, Chinese PLA General Hospital, Beijing, China

Contributions: (I) Conception and design: Z Guan; (II) Administrative support: B Xu; (III) Provision of study materials or patients: Z Guan; (IV) Collection and assembly of data: G Ma, J Du; (V) Data analysis and interpretation: G Ma, J Du; (VI) Manuscript writing: All authors; (VII) Final approval of manuscript: All authors.

[#]These authors contributed equally to this work.

Correspondence to: Zhiwei Guan. Department of Nuclear Medicine, Chinese PLA General Hospital, 28 Fuxing Road, Haidian District, Beijing 100853, China. Email: 13718806573@139.com.

Background: Pheochromocytomas/paragangliomas (PPGLs) predominantly express somatostatin receptors (SSTRs) 2 and 3. ^{68}Ga-DOTA(0)-Tyr(3)-octreotate (^{68}Ga-DOTA-TATE) is an imaging radiopharmaceutical that selectively targets SSTR 2 with high affinity. The purpose of this study was to evaluate the utility of ^{68}Ga-DOTA-TATE in the differential diagnosis of suspected PPGLs, and determine the optimal threshold for differential diagnoses.

Methods: This retrospective study reviewed consecutive patients referred to the Chinese PLA General Hospital, Beijing between April 2018 and December 2020 who underwent both biochemical testing for catecholamine and ^{68}Ga-DOTA-TATE positron emission tomography/computed tomography (PET/CT) for suspected PPGLs, without prior history. Patients with pathologic confirmation were selected for analysis. The following values were obtained for a quantitative analysis of ^{68}Ga-DOTA-TATE imaging: maximal standardized uptake value (SUV_{max}), the ratio between the SUV_{max} of the lesion and the mean SUV (SUV_{mean}) of the liver (SUVR), and the Krenning score (KS) of the lesion. According to their location, tumors were grouped as adrenal or extra-adrenal. Receiver operating characteristic (ROC) curves of the SUVR and KS were determined, and their diagnostic performance was calculated using general and subgroup-specific optimal thresholds. Concordance between the SUVR and KS was analyzed using a McNemar test.

Results: A total of 38 patients with PPGLs and 21 with non-PPGLs tumors were included in the final analysis. When a general optimal threshold for adrenal tumors was applied in pheochromocytoma (PCC) diagnosis, the sensitivity, specificity, and accuracy of the SUVR and KS were 86.4% (19/22) and 90.9% (20/22), 92.9% (13/14) and 78.6% (11/14), and 88.9% (32/36) and 86.1% (31/36), respectively. The SUVR and KS diagnostic results showed no differences in paraganglioma (PGL) diagnosis, with a sensitivity, specificity, and accuracy of 43.8% (7/16), 100.0% (7/7), and 60.9% (14/23), respectively. Using PPGL-specific optimal thresholds improved the diagnostic accuracy for extra-adrenal tumors. The diagnostic results of the SUVR and KS showed high concordance in both general and subgroup analyses. When PPGL-specific optimal thresholds were used, ^{68}Ga-DOTA-TATE PET/CT correctly diagnosed 1 PCC with negative biochemical test results, and 5 PCCs and 1 PGL with borderline biochemical test results.

Conclusions: Applying PPGL-specific thresholds of ^{68}Ga-DOTA-TATE in diagnosing adrenal and

extra-adrenal tumors is recommended for the differential diagnosis of PPGLs. When biochemical tests are negative or borderline, ^{68}Ga-DOTA-TATE PET/CT should be included in the diagnostic procedure. The visual KS method has almost the same diagnostic efficiency as the quantitative SUVR method and has potential for recommendation in ^{68}Ga-DOTA-TATE image analysis.

Keywords: ^{68}Ga-DOTA(0)-Tyr(3)-octreotate (^{68}Ga-DOTA-TATE); pheochromocytoma/paraganglioma (PPGL); positron emission tomography/computed tomography (PET/CT); differential diagnosis

Submitted Jun 21, 2021. Accepted for publication Dec 14, 2021.
doi: 10.21037/qims-21-652
View this article at: https://dx.doi.org/10.21037/qims-21-652

Introduction

Pheochromocytoma (PCC) and paraganglioma (PGL), collectively referred to as PPGL, belong to the same family of neural crest-derived neoplasms. The origin of PCCs is the adrenal medulla, while PGLs are extra-adrenal and originate from the sympathetic or parasympathetic paraganglia. These tumors are characterized by an excessive production of catecholamines, and the detection of excess catecholamines and their metabolites is the gold standard for diagnosing PPGLs (1). The role of whole-body (WB) PPGL-specific functional imaging is rapidly gaining prominence in precision medicine for patients with PPGLs, as these tumors are characterized by their multiplicity and wide distribution, and WB screening is routinely required for lesion detection. Notably, PPGLs express high levels of somatostatin receptors (SSTRs), particularly subtypes 2, 3, and 5 (2,3). Positron emission tomography (PET) imaging with ^{68}Ga-labeled DOTA-conjugated somatostatin analogues (^{68}Ga-DOTA-SSA) has shown excellent lesion-based accuracy in patients with PPGLs (4-7). According to a recent systematic review and meta-analysis (8), the pooled detection rate of ^{68}Ga-DOTA-SSA PET was 93% [95% confidence interval (CI): 91% to 95%], which was significantly higher than the detection rates of other functional imaging methods such as ^{18}F-fluoro-L-phenylalanine (^{18}F-FDOPA) PET [80% (95% CI: 69% to 88%)], ^{18}F-fluorodeoxyglucose (^{18}F-FDG) PET [74% (95% CI: 46% to 91%)], and $^{123/131}$I-labeled metaiodobenzylguanidine ($^{123/131}$I-MIBG) scans [38% (95% CI: 20% to 59%); P<0.001 for all]. It has also been shown that ^{68}Ga-DOTA-SSA PET detects more PPGL lesions than anatomical imaging (6,9).

Previous studies have usually focused on the performance of ^{68}Ga-DOTA-SST PET/computed tomography (CT) in detecting multiple lesions or metastatic foci in patients with confirmed PPGLs (4-7); however, information about ^{68}Ga-DOTA-SST PET/CT for differential diagnosis is scarce. When ^{68}Ga-DOTA-1-NaI3-octreotide (^{68}Ga-DOTA-NOC) PET/CT was used to diagnose PCC, the sensitivity, specificity, and accuracy were 90.4%, 85%, and 88.7%, respectively (10). Gild *et al.* reported the sensitivity of ^{68}Ga-DOTA(0)-Tyr(3)-octreotate (^{68}Ga-DOTA-TATE) PET/CT as 88% for PCC and 100% for PGL (11).

In a clinical setting, biochemical tests may fail to confirm or exclude the diagnosis of PPGLs on account of technical or tumor-related reasons (12). Where such uncertainty is present, ^{68}Ga-DOTA-SSA PET/CT would be relied on to confirm whether a tumor is a PPGL or not. Furthermore, tumors other than neuroendocrine tumors have been found to express varying amounts of SSTRs (13), so a specific ^{68}Ga-DOTA-SSA threshold for diagnosing PPGL is needed. In the case of ^{68}Ga-DOTA-NOC, a tumor maximal standardized uptake value (SUV_{max}) of the liver (SUV_{max}/SUV_{liver}) cutoff value of >2.5 showed the highest diagnostic accuracy [area under the curve (AUC) =0.741; 95% CI: 0.622 to 0.838] (10). For ^{68}Ga-DOTA-TATE, a SUV_{max} of >19.4 showed the highest diagnostic accuracy, reflecting a sensitivity of 63% and a specificity of 100% in differentiating PCC from adrenal adenoma (P=0.004) (11). Although previous reports (10,11) have provided valuable information, more research is undoubtedly needed. This study retrospectively reviewed a cohort of patients with suspected PPGLs to evaluate the efficiency of ^{68}Ga-DOTA-TATE PET/CT for differential diagnosis and to determine a specific ^{68}Ga-DOTA-TATE threshold for diagnosing PPGLs.

We present the following article in accordance with the Standards for Reporting of Diagnostic Accuracy (STARD) reporting checklist (available at https://qims.amegroups.com/article/view/10.21037/qims-21-652/rc).

Table 1 KSs

Uptake score	Relative uptake
0	Uptake ≤ blood pool
1	Uptake > blood pool but < physiologic liver uptake
2	Uptake similar as physiologic liver uptake
3	Uptake > physiologic liver uptake but < physiologic spleen uptake
4	Uptake ≤ physiologic spleen uptake

KSs, Krenning scores.

Methods

Patients

All procedures performed in this study involving human participants were conducted in accordance with the Declaration of Helsinki (as revised in 2013). The study was approved by the Ethics Committee of the Chinese PLA General Hospital. Individual consent for this retrospective analysis was waived.

In this study, we retrospectively reviewed consecutive patients referred to the Chinese PLA General Hospital between April 2018 and December 2020 who underwent both biochemical testing for catecholamine and ^{68}Ga-DOTA-TATE PET/CT for suspected PPGLs, without prior history. Histology results were considered the gold standard for final diagnosis. However, because the diagnosis of PPGLs relied on immunohistochemical (IHC) staining to differentiate them from other adrenal or retroperitoneal tumors, IHC staining results were also reviewed. Patients without histology results or IHC staining to confirm the diagnosis of PPGLs were excluded from the study.

We classified PPGLs as either adrenal PCC or PGL. A multifocal disease was defined as the coexistence of both types in the same patient. Malignancy was defined by the presence of metastases to sites that normally lack chromaffin tissue.

Biochemical tests

For the biochemical tests, blood was drawn in the supine position, with patients recumbent for at least 30 minutes before the blood sampling. Plasma-free metanephrine (pfMN), plasma-free normetanephrine (pfNMN), and 3-methoxytyramine (3-MT) were tested using a commercial enzyme immune assay kit manufactured by Labor Diagnostica (Nord GmbH, Nordhorn, Germany). The upper limits of the normal intervals for pfMN, pfNMN, and 3-MT were 420.9, 709.7, and 100 pmol/L, respectively. Biochemical test results were defined as positive if 1 of the biochemical results was 3-fold or more above the upper limits, and as borderline if 1 of the biochemical results was elevated to less than 3-fold above the upper limits. If within normal range, the biochemical test results were defined as negative. Any PPGLs with negative biochemical results were considered non-secretory tumors.

^{68}Ga-DOTA-TATE PET/CT acquisition and analysis

All PET/CT images were acquired on a hybrid PET/CT device [either a Biograph 64 with TrueV, Siemens Medical Systems (Siemens, Erlangen, Germany) or a Discovery 690 (GE Healthcare, Chicago, IL, USA)]. The injected dose of ^{68}Ga-DOTA-TATE was 130–185 MBq, with an uptake time of between 50 to 70 min. Patients were not required to fast for the study. Low-dose CT scans without the administration of a contrast agent were performed first. The PET acquisition protocol started with a WB acquisition from the base of the skull to the mid-thigh (3 minutes per bed position, arms above the head). The PET images were reconstructed using an iterative algorithm provided by the manufacturer. The low-dose CT scans were used for PET image attenuation correction and anatomical coregistration.

The ^{68}Ga-DOTA-TATE uptake of the tumors was visually graded and given a Krenning score (KS) (*Table 1*) (14,15). A score of 0 was defined as a negative result, while scores 1 to 4 were defined as a weak, moderate, strong, or very strong positive result, respectively.

The SUV_{max} for the lesions was obtained from volumes of interest (VOI). A two-dimensional (2D) VOI of 1 cm^2 was drawn at the site of the most intense uptake within the lesion on axial images, avoiding the intensity of the neighboring normal structures, especially when the lesions were located in the adrenal gland zone. In patients with bilateral PCCs, the PCC with the higher SUV_{max} was

included for analysis, while in patients with multifocal PPGLs, the tumor with the highest ^{68}Ga-DOTA-TATE uptake intensity was included for analysis, and the patient was classified into the corresponding subgroup. To reduce quantification variations caused by different radiopharmaceutical dosages or scan machines, we used the standardized uptake value ratio (SUVR). A 2D VOI of 1 cm^2 was drawn on the right lower segment of the liver to calculate the mean SUV (SUV_{mean}). The SUVR was defined and calculated as the ratio between the SUV_{max} of the lesion and the SUV_{mean} of the liver. Image readers were blinded to the patients' clinical information and histological results.

Statistical analysis

For statistical analysis, we used the software SPSS 21.0 (IBM Corp., Armonk, NY, USA). The sample profile was described according to the variables under scrutiny. For categorical variables, we used frequency tables with an absolute frequency (n) and percentage (%). For numerical variables, we used descriptive statistics with mean, standard deviation, minimum, maximum, and median values. Continuous variables were tested for normality, and an independent *t*-test or non-parametric Mann-Whitney U-test was used for intergroup comparisons. For categorical variables, comparisons were made using a chi-square or non-parametric Mann-Whitney U-test. Receiver operating characteristic (ROC) curves and Youden's J statistic were used to determine the optimal SUVR and KS values for PPGL diagnosis. Diagnostic agreement between the two methods was compared pairwise using a McNemar test and kappa statistics. Comparisons and ROC analyses were also performed among tumor subgroups. For the comparative study, PPGLs were classified into either a PCC or a PGL subgroup, while for the ROC analyses, the tumors were classified into either an adrenal or an extra-adrenal lesion subgroup. A P value <0.05 was regarded statistically significant.

Results

Patient and tumor characteristics

Among the patients reviewed, a final diagnosis was established for 59 cases, and these were selected for the subsequent analyses. The time interval between the ^{68}Ga-DOTA-TATE PET/CT and histologic results was 1–6 weeks. Patient characteristics are listed in *Table 2*. There were 21 cases with non-PPGL tumors and 38 cases with PPGLs, including 21 with PCC, 14 with PGL, and 3 with multifocal PPGLs. There were no significant differences between the gender and ages of the PPGL and non-PPGL groups. According to the clinical findings, 4 cases were identified as having multiple endocrine neoplasia type 2 (MEN2) syndrome, and 2 cases had von Hippel-Lindau (VHL) syndrome. Among these cases, 3 underwent genetic testing to confirm the diagnosis. Genetic testing showed a *SDHD* mutation in another patient who had bilateral PCCs, a retroperitoneal PGL, and a head and neck (HN)-PGL. The genetic status of other patients was unknown. In total, 5 cases had bilateral PCCs, and 2 had malignant PPGLs, as both were found to have multiple metastatic pulmonary nodules in the ^{68}Ga-DOTA-TATE PET/CT images. The pathology of non-PPGL tumors covered a wide range, from benign to malignant (*Table 2*). The most frequent pathologic types of non-PPGL tumors were peripheral nerve sheath tumors (PNSTs) (6 cases) and adrenocortical adenomas (AAs) (4 cases). Of the non-PPGL tumors, 3 were malignant, including 2 adrenocortical carcinomas

Table 2 Patient and tumor characteristics

Characteristics	PPGLs	Non-PPGL tumors	Statistical value
Age (years)			t=−0.630, P=0.532
Median	40.5	52	
Range	16–74	15–83	
Gender, n (%)			χ^2=0.011, P=0.917
Male	23 (60.5)	13 (61.9)	
Female	15 (39.5)	8 (38.1)	

Table 2 (*continued*)

Table 2 (*continued*)

Characteristics	PPGLs	Non-PPGL tumors	Statistical value
Site of analyzed lesion, n (%)			χ^2=0.438, P=0.508
PCC	22 (57.9)	–	
Retroperitoneal PGL	15 (42.1)	–	
Mediastinal PGL	1	–	
Adrenal gland	–	14 (66.7)	
Retroperitoneal	–	7 (33.3)	
Tumor size analyzed (mm)			t=–0.230, P=0.819
Median	45	47	
Range	19–189	21–189	
Biochemical tests			Z=–6.558, P=0.001
Positive	30	0	
Borderline	6	1	
Negative	2	20	
Mutation			
SDHD	1	–	
VHL	2	–	
RET	4	–	
Unknown	32	–	
Pathology			
PNST	–	6	
AA	–	4	
Ganglioneuroma	–	2	
Hemolymphangioma	–	2	
Adenoid tumor of adrenal gland	–	1	
GIST	–	1	
Angiomyolipoma	–	1	
RSF	–	1	
AC	–	2	
Metastasis of RCC	–	1	
SUV_{max} of the tumor	22.6±16.1	4.6±3.3	Z=–5.098, P=0.001
SUV_{mean} in liver	10.4±2.1	10.1±2.4	t=0.588, P=0.559
SUVR of the tumor	2.3±1.7	0.5±0.4	Z=–4.894, P=0.001
KS (grade/number)	0/0, 1/11, 2/4, 3/7, 4/16	0/10, 1/8, 2/3, 3/0, 4/0	Z=–5.163, P=0.001

PPGLs, pheochromocytomas/paragangliomas; PCC, pheochromocytoma; PGL, paraganglioma; VHL, von Hippel-Lindau syndrome; PNST, peripheral nerve sheath tumor; AA, adrenocortical adenoma; GIST, gastrointestinal stroma tumor; RSF, retroperitoneal solitary fibroma; AC, adrenocortical carcinoma; RCC, renal cell carcinoma; SUV_{max}, maximal standardized uptake value; SUV_{mean}, mean standardized uptake value; SUVR, ratio between the SUV_{max} of the lesion and the SUV_{mean} of the liver; KS, Krenning score.

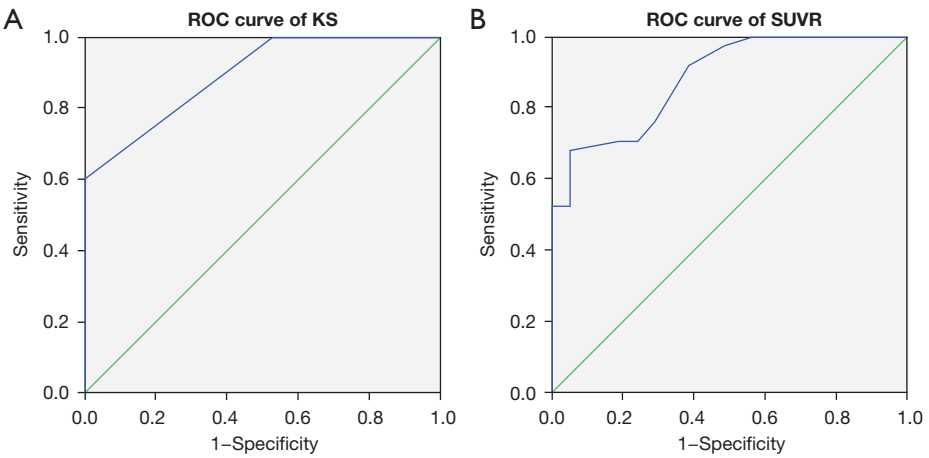

Figure 1 ROC curve for ^{68}Ga-DOTA-TATE PET/CT in general. (A) AUC of SUVR was 0.887 (95% CI: 0.804 to 0.969). (B) AUC of KS was 0.896 (95% CI: 0.819 to 0.973). ROC, receiver operating characteristic; ^{68}Ga-DOTA-TATE, ^{68}Ga-DOTA(0)-Tyr(3)-octreotate; AUC, area under the curve; SUVR, ratio between the SUV_{max} of the lesion and the SUV_{mean} of the liver; SUV_{max}, maximal standardized uptake value; SUV_{mean}, mean standardized uptake value; KS, Krenning scale; CI, confidence interval.

(ACs) and 1 metastasis of renal cell carcinoma (RCC). Some pathologic types of the adrenal tumors were very rare, such as hemolymphangioma (n=2) and adenomatoid tumor of the adrenal gland (n=1 patient).

Biochemical test results

A total of 30 patients returned positive biochemical results, while 7 were borderline, and 22 were negative (*Table 2*). All cases with positive biochemical results had PPGLs, while those with borderline biochemical results included 5 PCC patients, 1 PGL patient, and 1 non-PPGL tumor patient. There were 2 PCC patients who returned negative biochemical results. Among the non-PPGL tumor patients, only 1 with an adenomatoid tumor of the adrenal gland returned borderline biochemical results. With a diagnosis of PPGL based on the positive biochemical results, the sensitivity, specificity, positive predictive value (PPV), negative predictive value (NPV), and accuracy were 78.9% (30/38), 95.2% (20/21), 100.0% (30/30), 72.4% (21/29), and 86.4% (51/59), respectively.

^{68}Ga-DOTA-TATE PET/CT diagnostic accuracy in general analysis

All the PPGL lesions included in the analysis were positive on the ^{68}Ga-DOTA-TATE PET/CT images, but the uptake intensity varied from weak to very strong. Of the 21 non-PPGL tumors, 11 showed positive uptake, but the intensity was weak (8 tumors) or moderate (3 tumors). The SUV_{max}, SUVR, and KS of the PPGLs were all significantly higher than in the non-PPGL tumors, though there was no significant difference between the tumor sizes in the two groups (*Table 2*).

First, we performed a general ROC analysis that included all the PPGLs. The AUC of the SUVR was 0.887 (95% CI: 0.804 to 0.969) (*Figure 1A*). With a general optimal cutoff value of 1.05, the SUVR correctly diagnosed 26 PPGLs and 20 non-PPGL tumors, with a sensitivity, specificity, PPV, NPV, and accuracy of 68.4% (26/38), 95.7% (20/21), 96.3% (26/27), 62.5% (20/32), and 78.0% (46/59), respectively (*Table 3*).

The AUC of the KS was 0.896 (95% CI: 0.819 to 0.973) (*Figure 1B*), and grade 2 was chosen as the general optimal KS cutoff value. A diagnosis of PPGL was made if the KS ≥ grade 2, and the KS correctly diagnosed 27 PPGLs and 18 non-PPGL tumors, with a sensitivity, specificity, PPV, NPV, and accuracy of 71.0% (27/38), 85.7% (18/21), 90.0% (27/30), 62.1% (18/29), and 76.3% (45/59), respectively (*Table 3*). A McNemar test indicated that the diagnostic results of the two methods were not significantly different (P=0.250). In fact, the results compared pairwise were in high concordance (Kappa =0.898). Diagnostic differences occurred in only 3 adrenal tumors, including 2 non-PPGL tumors which were misdiagnosed by the KS, and 1 PCC tumor which was misdiagnosed by the SUVR.

Table 3 Efficiency of ^{68}Ga-DOTA-TATE PET/CT in the differential diagnosis of all PPGLs

Methods	Sensitivity	Specificity	Accuracy	PPV	NPV
SUVR	68.4% (26/38)	95.7% (20/21)	78.0% (46/59)	96.3% (26/27)	62.5% (20/32)
KS	71.0% (27/38)	85.7% (18/21)	76.3% (45/59)	90.0% (27/30)	62.1% (18/29)

^{68}Ga-DOTA-TATE, ^{68}Ga-DOTA(0)-Tyr(3)-octreotate; PET/CT, positron emission tomography/computed tomography; PPGLs, pheochromocytomas/paragangliomas; PPV, positive predictive value; NPV, negative predictive value; SUVR, ratio between the SUV_{max} of the lesion and the SUV_{mean} of the liver; SUV_{max}, maximal standardized uptake value; SUV_{mean}, mean standardized uptake value; KS, Krenning score.

Table 4 Comparison between PCC and PGL tumors

Characteristics	PCC	PGL	Statistical value
Number	22	16	
Tumor size (mm), mean ± SD	38.8±20.5	74.0±40.0	Z=−3.357, P=0.001
SUV_{max}	30.6±16.2	11.7±7.2	Z=−3.755, P=0.000
SUVR	3.1±1.7	1.1±0.7	Z=−3.631, P=0.000
KS			Z=−3.081, P=0.002
0	0	0	
1	2	9	
2	1	3	
3	6	1	
4	13	3	

PCC, pheochromocytoma; PGL, paraganglioma; SUV_{max}, maximal standardized uptake value; SUVR, ratio between the SUV_{max} of the lesion and the SUV_{mean} of the liver; SUV_{mean}, mean standardized uptake value; KS, Krenning score.

Comparison between PCCs and PGLs

Among the PPGL group, 3 cases had multifocal tumors. Of these, 1 patient was grouped as PCC, and 2 as PGL according to the lesions with the highest ^{68}Ga-DOTA-TATE uptake. Consequently, the PCC group included 22 patients and the PGL group included 16. The tumor characteristics of the two groups were different (*Table 4*). The PGLs were bigger, but the uptake of these tumors, measured as the SUV_{max}, SUVR, or KS, was significantly less than the uptake of the PCCs. We grouped the tumors included in our analysis as adrenal or extra-adrenal according to their location. We used ^{68}Ga-DOTA-TATE PET/CT for PCC diagnosis in adrenal tumors and for PGL diagnosis in extra-adrenal tumors. The diagnostic results of the SUVR and the KS were different in 3 adrenal tumors. The sensitivity, specificity, PPV, NPV, and accuracy of the SUVR and the KS were 86.4% (19/22) and 90.9% (20/22), 92.9% (13/14) and 78.6% (11/14), 95% (19/20) and 87.0% (20/23), 81.2% (13/16) and 84.6% (11/13), and 88.9% (32/36) and 86.1% (31/36), respectively (*Table 5*). The diagnostic results of the SUVR and the KS showed no difference in extra-adrenal tumors with a sensitivity, specificity, PPV, NPV, and accuracy of 43.8% (7/16), 100% (7/7), 100% (7/7), 43.8% (7/16), and 60.9% (14/23), respectively (*Table 5*). Both the SUVR and the KS correctly diagnosed more PCCs than PGLs (χ^2=7.785, P=0.005; χ^2=10.016, P=0.002, respectively).

ROC subgroup analysis for adrenal and extra-adrenal tumors

We then performed ROC analyses of the adrenal and extra-adrenal subgroups to define subgroup-specific optimal SUVR and KS cut-off values for diagnosing PCC or PGL. For the adrenal tumor subgroup, the optimal SUVR and KS cut-off values for PCC diagnosis were 1.15 and grade 2, respectively, and the AUCs were 0.942 (95% CI: 0.87 to 1.000) and 0.956 (95% CI: 0.895 to 1.000), respectively (*Figure 2A*,*2B*). When these subgroup-specific optimal

Table 5 Efficiency of ^{68}Ga-DOTA-TATE PET/CT in the differential diagnosis of PCC and PGL using the general optimal cutoff values

Groups	Sensitivity	Specificity	Accuracy	PPV	NPV
PCC					
SUVR	86.4% (19/22)	92.9% (13/14)	88.9% (32/36)	95.0% (19/20)	81.2% (13/16)
KS	90.9% (20/22)	78.6% (11/14)	86.1% (31/36)	87.0% (20/23)	84.6% (11/13)
PGL					
SUVR	3.8% (7/16)	100.0% (7/7)	60.9% (14/23)	100.0% (7/7)	43.8% (7/16)
KS	43.8% (7/16)	100.0% (7/7)	60.9% (14/23)	100.0% (7/7)	43.8% (7/16)

^{68}Ga-DOTA-TATE, ^{68}Ga-DOTA(0)-Tyr(3)-octreotate; PET/CT, positron emission tomography/computed tomography; PCC, pheochromocytoma; PGL, paraganglioma; PPV, positive predictive value; NPV, negative predictive value; SUVR, ratio between the SUV_{max} of the lesion and the SUV_{mean} of the liver; SUV_{max}, maximal standardized uptake value; SUV_{mean}, mean standardized uptake value; KS, Krenning score.

cut-off values were applied, the diagnostic results of the SUVR and KS in diagnosing PCC were same as the results produced using the previously described general optimal cut-off values. For the extra-adrenal tumor subgroup, the optimal cut-off values of the SUVR and KS for PGL diagnosis were changed to 0.55 and grade 1, respectively, and the AUCs were 0.906 (95% CI: 0.751 to 1.000) and 0.920 (95% CI: 0.791 to 1.000) (*Figure 2C*,*2D*). Using the subgroup-specific optimal SUVR and KS cut-off values improved the diagnostic accuracy for extra-adrenal tumors compared to using the general optimal cut-off values. The diagnostic results of the SUVR and KS were different, though not significantly so, for 3 patients in the extra-adrenal tumor subgroup (McNemar P=0.250). The sensitivity, specificity, PPV, NPV, and accuracy were 87.5% (14/16) and 100% (16/16), 100% (7/7) and 71.4% (5/7), 93.3% (14/15) and 88.9% (16/18), 75.0% (6/8) and 100% (5/5), and 90.1% (20/23) and 91.3% (21/23), respectively (*Table 6*).

False positive and false negative uptake of ^{68}Ga-DOTA-TATE

When the general optimal cut-off value was applied in diagnosis, false positive uptake of ^{68}Ga-DOTA-TATE occurred only in adrenal tumors. According to the KS, 2 adrenal adenomas and an adenomatoid tumor of the adrenal gland were false positives, while the SUVR correctly diagnosed all 3 tumors. There were a higher number of false negatives. According to the KS, 2 PCCs and 9 PGLs were false negatives, while 1 more PCC was a false negative according to the SUVR. Subgroup-specific optimal cut-off values improved the diagnostic accuracy for PGLs. According to the SUVR, only 2 PGLs were false negatives and only a PNST was a false positive. The KS diagnosed all PGLs correctly, but 2 tumors (a PNST and an angiomyolipoma at the renal portal zone) were false positives.

Patients with PPGL and negative or borderline biochemical results

Finally, we applied the subgroup-specific optimal cut-off values for final diagnosis. For the 2 PCC patients with negative biochemical results, 1 was correctly diagnosed by ^{68}Ga-DOTA-TATE PET/CT (*Figure 3*). For the 7 patients with borderline biochemical results, ^{68}Ga-DOTA-TATE PET/CT correctly diagnosed all PPGLs, including 5 PCCs and 1 PGL. The only non-PPGL tumor with borderline biochemical results was a false positive visually, but was correctly diagnosed with the SUVR (*Figure 4*). By combining biochemical tests and ^{68}Ga-DOTA-TATE PET/CT in the diagnostic procedure, 97.4% (37/38) of the PPGLs were correctly diagnosed.

Discussion

In the present study, we evaluated the performance of ^{68}Ga-DOTA-TATE PET/CT in differentiating PPGLs from non-PPGL tumors. We analyzed the PET/CT images using both a visual and quantitative method. We used the SUVR rather than the SUV_{max}, because the SUVR took hepatic accumulation as the internal reference, possibly reducing the quantification variations caused by radiopharmaceutical dosage or different scan machines. The KS also took hepatic accumulation as the internal reference. The KS

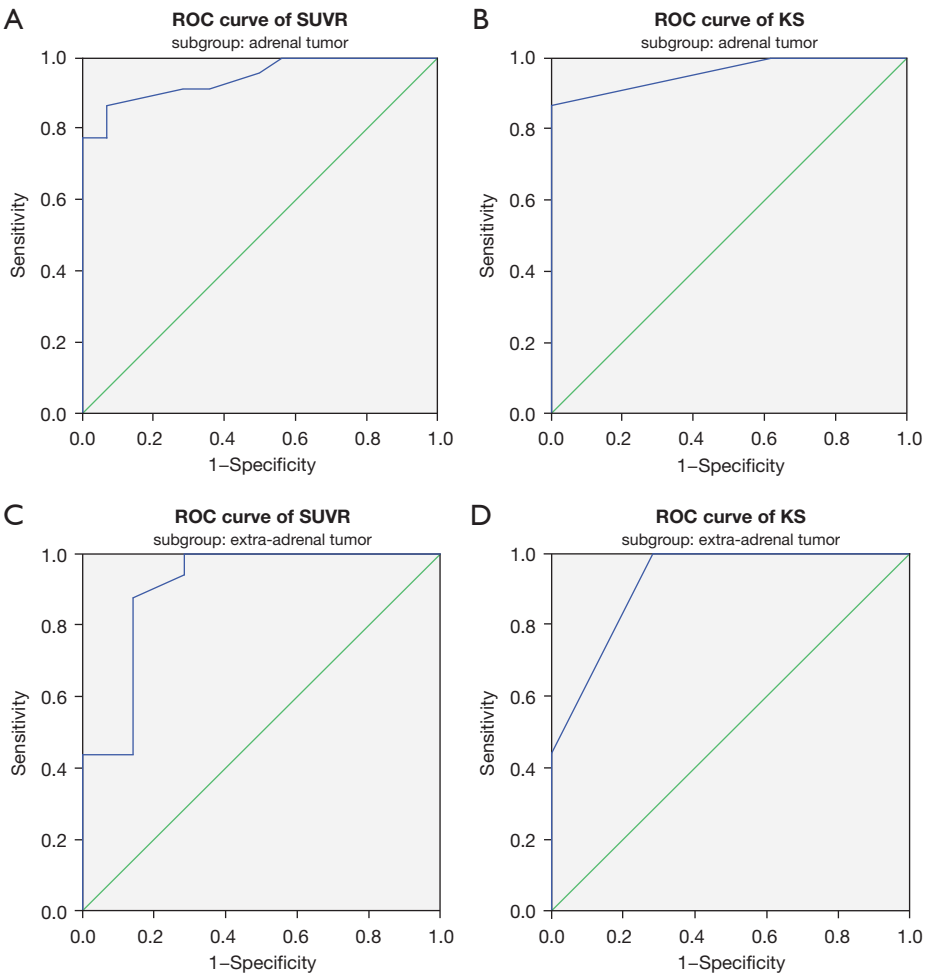

Figure 2 ROC curve for ^{68}Ga-DOTA-TATE PET/CT in subgroups of adrenal tumor (A,B) and extra-adrenal tumor (C,D). (A) In adrenal tumor, the AUC of SUVR was 0.942 (95% CI: 0.87 to 1.000). (B) In adrenal tumor, AUC of score of KS was 0.956 (95% CI: 0.895 to 1.000). (C) In extra-adrenal tumor, AUC of SUVR was 0.906 (95% CI: 0.751 to 1.000). (D) In extra-adrenal tumor, AUC of KS was 0.920 (95% CI: 0.791 to 1.000). ROC, receiver operating characteristic; ^{68}Ga-DOTA-TATE, ^{68}Ga-DOTA(0)-Tyr(3)-octreotate; PET/CT, positron emission tomography/computed tomography; AUC, area under the curve; SUVR, ratio between the SUV_{max} of the lesion and the SUV_{mean} of the liver; SUV_{max}, maximal standardized uptake value; SUV_{mean}, mean standardized uptake value; KS, Krenning scale; CI, confidence interval.

was first used to interpret the octreoscans of patients with PPGLs. Obtained visually and conveniently, the KS and modified KS are widely used in interpreting ^{68}Ga-DOTA-TATE PET/CT images to select candidates for SSTR-target radioisotope therapy. However, their utility in ^{68}Ga-DOTA-TATE PET/CT image interpretation for PPGL diagnosis has not been verified. In our study, both the KS and SUVR indicated varying expression levels of SSTR2 in the primary PPGLs, which was consistent with previous *in vitro* findings. Leijon *et al.* and Elston *et al.* semi-quantitatively analyzed the SSTR immunostaining profile of resected PPGLs (3,16) and found that the expression of SSTR2 varied from negative to strong in these tumors. In our study, we found that about half of the non-PPGL tumors also absorbed ^{68}Ga-DOTA-TATE, with uptake varying from weak to moderate.

Considering that both PPGL and non-PPGL tumors express varying levels of SSTR2, we believed it preferable to quantify the uptake of ^{68}Ga-DOTA-TATE and define an optimal threshold for specific diagnostic purposes. Previous studies have usually analyzed the ^{68}Ga-DOTA-TATE PET/CT image visually but seldom quantified or

Table 6 Efficiency of ^{68}Ga-DOTA-TATE PET/CT in differential diagnosis of PCC and PGL using subgroup-specific optimal cutoff values

Subgroups	Sensitivity	Specificity	Accuracy	PPV	NPV
PCC					
SUVR	86.4% (19/22)	92.9% (13/14)	88.9% (32/36)	95.0% (19/20)	81.2% (13/16)
KS	90.9% (20/22)	78.6% (11/14)	86.1% (31/36)	87.0% (20/23)	84.6% (11/13)
PGL					
SUVR	87.5% (14/16)	100.0% (7/7)	90.1% (20/23)	93.3% (14/15)	75.0% (6/8)
KS	100.0% (16/16)	71.4% (5/7)	91.3% (21/23)	88.9% (16/18)	100.0% (5/5)

^{68}Ga-DOTA-TATE, ^{68}Ga-DOTA(0)-Tyr(3)-octreotate; PET/CT, positron emission tomography/computed tomography; PCC, pheochromocytoma; PGL, paraganglioma; PPV, positive predictive value; NPV, negative predictive value; SUVR, ratio between the SUV_{max} of the lesion and the SUV_{mean} of the liver; SUV_{max}, maximal standardized uptake value; SUV_{mean}, mean standardized uptake value; KS, Krenning score.

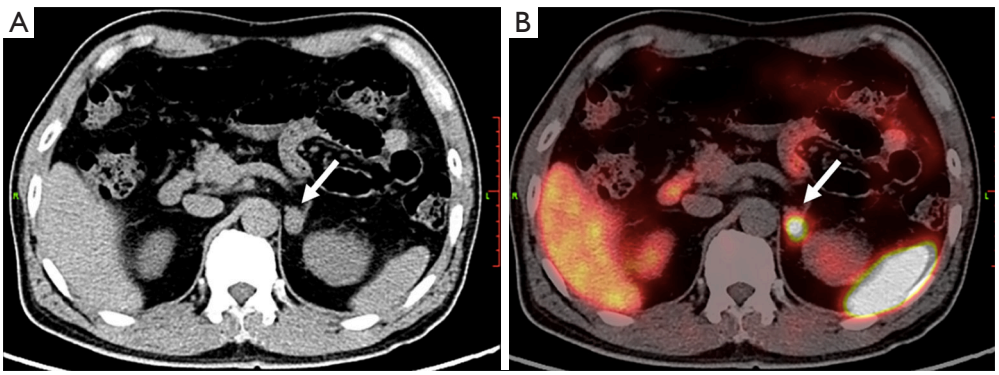

Figure 3 PCC in a 66-year-old male. (A) CT image showing a hypointense tumor at the left adrenal gland (arrow). Biochemical tests of functional adrenal tumors including PPGLs were all negative. (B) This tumor showed intense uptake of ^{68}Ga-DOTAT-TATE in the CT and PET fusion image (arrow). The SUV_{max} was 19.1, SUVR was 2.2, score of KS was 3 respectively. PCC was diagnosed before surgery, and was later confirmed by histologic results. PCC, pheochromocytoma; CT, computed tomography; PPGLs, pheochromocytomas/paragangliomas; ^{68}Ga-DOTA-TATE, ^{68}Ga-DOTA(0)-Tyr(3)-octreotate; PET, positron emission tomography; SUV_{max}, maximal standardized uptake value; SUVR, ratio between the SUV_{max} of the lesion and the SUV_{mean} of the liver; SUV_{mean}, mean standardized uptake value; KS, Krenning scale.

defined uptake levels for diagnostic purposes. In our study, we first defined a general optimal threshold for differential diagnosis by ROC analysis for all the cases. With this general optimal threshold, the sensitivity and specificity of the SUVR and KS were 68.4% (26/38) and 71.0% (27/38), and 95.7% (20/21) and 85.7% (18/21), respectively. Overall, ^{68}Ga-DOTA-TATE PET/CT was not sensitive enough to differentiate between PPGL and non-PPGL tumors. We analyzed the PCC and PGL data separately, and found that PCCs uptake significantly more ^{68}Ga-DOTA-TATE than PGLs. As a result, ^{68}Ga-DOTA-TATE PET/CT using the general threshold was more sensitive in diagnosing PCCs than PGLs (*Table 4*). Once this finding was established, the location of the PGLs needed to be considered. There are distinct differences between HNPGLs and retroperitoneal PGLs. The HNPGLs uptake ^{68}Ga-DOTA-TATE avidly, and higher detection rates have been reported in studies that showed a greater prevalence of HNPGLs (5,9). The PGLs included in our study were all retroperitoneal, except for 1 located in the mediastinum. Retroperitoneal PGLs are usually large and degenerated. Degenerative photopenia in ^{68}Ga-DOTA-TATE PET/CT images was found in all the retroperitoneal PGLs, and might be an important reason for the false negative results in our study. Gild *et al.* also evaluated the role of ^{68}Ga-DOTA-TATE PET/CT in the preoperative assessment of suspected PPGLs (11). Their study showed that the sensitivity of ^{68}Ga-DOTA-TATE PET/CT in diagnosing primary PCCs and PGLs was 88%

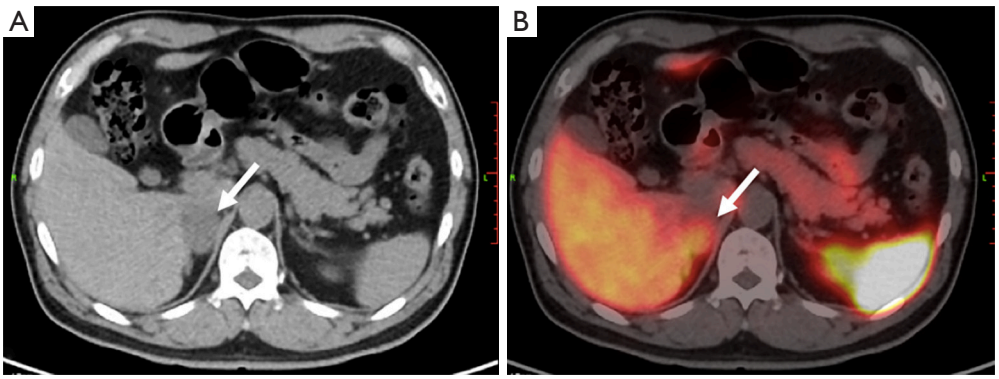

Figure 4 Adenomatoid tumor of adrenal gland in a 63-year-old male. His pfNMN was 476.3pmol/L, slightly above the normal range, and was defined as borderline. (A) Axial CT image shows a hypointense tumor at the right adrenal gland (arrow). (B) The tumor shows a moderate uptake of ^{68}Ga-DOTA-TATE in the CT and PET fusion image (arrow). The SUV_{max} was 10.2, SUVR was 0.9, and KS score was 2. This tumor was diagnosed as PCC visually before surgery. Histologic results after surgery indictaed an adenomatoid tumor of the adrenal gland. pfNMN, plasma-free normetanephrine; CT, computed tomography; ^{68}Ga-DOTA-TATE, ^{68}Ga-DOTA(0)-Tyr(3)-octreotate; PET, positron emission tomography; SUV_{max}, maximal standardized uptake value; SUVR, ratio between the SUV_{max} of the lesion and the SUV_{mean} of the liver; SUV_{mean}, mean standardized uptake value; KS, Krenning scale; PCC, pheochromocytoma.

and 100%, respectively. Although their results are different to ours, the location of the PGLs in their study was not mentioned, and the patient numbers for PGL (7 patients) and non-PGL (1 patient) were small.

Due to the significantly different uptake levels in PCCs and PGLs, we considered it better to perform subgroup ROC analyses to define specific SUVR and KS cut-off values. Therefore, we grouped the tumors into either an adrenal or an extra-adrenal subgroups according to their location. In the general ROC analysis, the optimal cutoff values were 1.05 for the SUVR and grade 2 for the KS. In the adrenal tumor subgroup analysis, the optimal cutoff values were 1.15 for the SUVR and grade 2 for the KS. As these values were almost the same as the general cutoff values, there were no diagnostic changes in this subgroup. In the extra-adrenal tumor subgroup, the optimal cutoff value was 0.55 for the SUVR and grade 1 for the KS. When these subgroup-specific optimal cutoff values were applied, more PGLs were correctly diagnosed. Diagnostic accuracy improved from 60.9% to 91.3%, indicating that a subgroup-specific optimal cutoff value was more effective for PGL diagnosis. Based on our data, we recommend that location-specific cutoff values be applied in diagnosing adrenal and extra-adrenal tumors.

In our study, we interpreted the ^{68}Ga-DOTA-TATE PET/CT images visually and quantitatively. The quantitative method used to be considered more accurate than the visual method. Therefore, we sought to determine whether the visual KS method was as reliable as the quantitative SUVR method in diagnostic work. We compared the diagnostic results of the KS with those of the SUVR, and found that they were in high concordance in both the general and subgroup-specific analyses. In the general study, the optimal cutoff values were 1.05 for the SUVR and grade 2 for the KS, both indicating that an uptake intensity equal or similar to hepatic accumulation was the optimum threshold for differential diagnosis. In the subgroup-specific analysis, the individual cutoff values for the SUVR and KS were also in concordance. The optimal cutoff values in the adrenal tumor subgroup were 1.15 for the SUVR and grade 2 for the KS. The optimal cutoff values in the extra-adrenal tumor subgroup were 0.55 for the SUVR and grade 1 for the KS. Agreement between the SUVR and KS was verified by the diagnostic results. As the KS was visually graded, and the SUV_{mean} of ^{68}Ga-DOTA-TATE in the liver was very high, tumors given the same KS scores may have had different SUVR values. In this case, there may have been discrepancies between the diagnostic results of the SUVR and the KS (*Figure 4*). In fact, in our general analysis, 3 adrenal tumors were differently diagnosed, while in our subgroup-specific analyses, 3 adrenal tumors and 3 extra-adrenal tumors were differently diagnosed. However, a McNemar test showed that the differences were not significant. Therefore, the differential efficiency of the KS was similar to that of the SUVR. Considering its convenience, the KS could be

recommended for ^{68}Ga-DOTA-TATE PET/CT image interpretation in PPGL diagnosis. Recently, 177Lu-DOTA-TATE has been used to treat patients with locally invasive and/or metastatic PPGLs (17), and the KS has been used to interpret ^{68}Ga-DOTA-TATE PET/CT images and select candidates for SSTR2-targeting peptide receptor radionuclide therapy (PRRT). This also suggests that the KS is useful in ^{68}Ga-DOTA-TATE image interpretation for patients with PPGLs.

AAs have been reported to yield false positives in ^{68}Ga-DOTA-NOC PET/CT images (10). According to previous histology studies, most cortical adenomas are positive for all 5 subtypes of SSTR (18). Therefore, false positive cortical adenomas may occur in ^{68}Ga-DOTA-SSA PET/CT images. In our study, visual interpretation returned false positives for 2 AAs and an adenomatoid tumor of the adrenal gland. The SUVR correctly diagnosed the same 3 adrenal tumors, indicating that SUVR was more accurate in non-PCC diagnosis. Both PCCs and PGLs could return false negatives in ^{68}Ga-DOTA-TATE PET/CT images. Degenerative photopenia featured in ^{68}Ga-DOTA-TATE PET/CT images and might have been an important reason for a false negative result. If a tumor was suspected of being a PGL, a grade 1 KS, rather than a grade 2, was recommended as the optimal threshold for diagnosis.

Biochemical testing for pfMN has proven highly accurate in diagnosing PPGLs (19); however, the accuracy of biochemical testing may be affected by sampling or measuring techniques (12). A large problem for interpreting test results involves those that are borderline, which constitute a quarter of all patients with PPGLs and a much larger proportion of patients without PPGL tumors but with similarly elevated test results (20). Our data showed the value of ^{68}Ga-DOTA-TATE PET/CT in diagnosing PPGLs with negative or borderline biochemical test results. In clinical scenarios with suspected PPGL but negative or borderline biochemical test results, a ^{68}Ga-DOTA-TATE PET/CT scan is necessary. An interesting case in our study, due to its rarity, was an adenomatoid tumor of the adrenal gland. Cases reported in the literature have shown the tumor as non-functioning (21,22), but the patient in our study returned borderline biochemical test results, and a PCC was suspected. The tumor showed a grade 2 uptake of ^{68}Ga-DOTA-TATE (*Figure 4*), and was visually positive. This case suggested that this rare tumor also expresses SSTR2 and could produce a false positive result, mimicking a PCC in ^{68}Ga-DOTA-TATE PET/CT images.

Our study had certain limitations. This was a retrospective analysis and included a relatively small patient population, due to the rarity of the disease. Though genetic testing was recommended for all patients with PPGLs, the fees are high, and not covered by Medicare in China mainland, so the genetic status of most patients remained unknown. As a result, we could not evaluate the effect of the patients' genetic status on ^{68}Ga-DOTA-TATE uptake, or on the differential efficiency of ^{68}Ga-DOTA-TATE PET/CT for suspected PPGLs. We did not evaluate the efficiency of ^{68}Ga-DOTA-TATE PET/CT in lesion detection, which is the most frequent indication for ^{68}Ga-DOTA-TATE PET/CT imaging in clinical use. However, there have been many previous studies, and data is abundant in this field. Finally, the optimal ROC thresholds might have been affected by the cohort size. The cohort in this study was relatively large for the general analysis, but for the subgroup analyses, the cohorts became relatively small. Moreover, this was a single-center study. The SUVR might be affected by machines or imaging techniques in different hospitals. Whether the SUVR and KS cut-off values translate successfully to other hospitals requires further research.

Conclusions

The uptake of ^{68}Ga-DOTA-TATE is significantly different between primary PCCs and retroperitoneal PGLs. Using specific thresholds of ^{68}Ga-DOTA-TATE for diagnosing PCCs and PGLs improves diagnostic performance and thus is recommended. For the differential diagnosis of suspected PPGLs, the quantitative SUVR method and the visual KS method were almost equally efficient. Considering the convenience of the KS and its value in candidate selection for PRRT, KS is recommended for clinical PPGL diagnosis. Using ^{68}Ga-DOTA-TATE PET/CT helps to diagnose PPGLs that return negative or borderline biochemical test results. Therefore, ^{68}Ga-DOTA-TATE PET/CT should be included in the diagnostic procedure of PPGLs when biochemical test results are negative or borderline.

Acknowledgments

Funding: This study was supported by the National Clinical Research Center for Geriatric Disease, Chinese PLA General Hospital (No. NCRCG-PLAGH-2019012).

Footnote

Reporting Checklist: The authors have completed the STARD

reporting checklist. Available at https://qims.amegroups.com/article/view/10.21037/qims-21-652/rc

Conflicts of Interest: All authors have completed the ICMJE uniform disclosure form (available at https://qims.amegroups.com/article/view/10.21037/qims-21-652/coif). The authors have no conflicts of interest to declare.

Ethical Statement: The authors are accountable for all aspects of the work in ensuring that questions related to the accuracy or integrity of any part of the work are appropriately investigated and resolved. All procedures performed in this study involving human participants were conducted in accordance with the Declaration of Helsinki (as revised in 2013). The study was approved by the Ethics Committee of the Chinese PLA General Hospital. Individual consent for this retrospective analysis was waived.

References

1. Lenders JW, Duh QY, Eisenhofer G, Gimenez-Roqueplo AP, Grebe SK, Murad MH, Naruse M, Pacak K, Young WF Jr; Endocrine Society. Pheochromocytoma and paraganglioma: an endocrine society clinical practice guideline. J Clin Endocrinol Metab 2014;99:1915-42.
2. Mundschenk J, Unger N, Schulz S, Höllt V, Schulz S, Steinke R, Lehnert H. Somatostatin receptor subtypes in human pheochromocytoma: subcellular expression pattern and functional relevance for octreotide scintigraphy. J Clin Endocrinol Metab 2003;88:5150-7.
3. Leijon H, Remes S, Hagström J, Louhimo J, Mäenpää H, Schalin-Jäntti C, Miettinen M, Haglund C, Arola J. Variable somatostatin receptor subtype expression in 151 primary pheochromocytomas and paragangliomas. Hum Pathol 2019;86:66-75.
4. Maurice JB, Troke R, Win Z, Ramachandran R, Al-Nahhas A, Naji M, Dhillo W, Meeran K, Goldstone AP, Martin NM, Todd JF, Palazzo F, Tan T. A comparison of the performance of ^{68}Ga-DOTATATE PET/CT and ^{123}I-MIBG SPECT in the diagnosis and follow-up of phaeochromocytoma and paraganglioma. Eur J Nucl Med Mol Imaging 2012;39:1266-70.
5. Archier A, Varoquaux A, Garrigue P, Montava M, Guerin C, Gabriel S, Beschmout E, Morange I, Fakhry N, Castinetti F, Sebag F, Barlier A, Loundou A, Guillet B, Pacak K, Taïeb D. Prospective comparison of (68)Ga-DOTATATE and (18)F-FDOPA PET/CT in patients with various pheochromocytomas and paragangliomas with emphasis on sporadic cases. Eur J Nucl Med Mol Imaging 2016;43:1248-57.
6. Janssen I, Chen CC, Millo CM, Ling A, Taieb D, Lin FI, Adams KT, Wolf KI, Herscovitch P, Fojo AT, Buchmann I, Kebebew E, Pacak K. PET/CT comparing (68)Ga-DOTATATE and other radiopharmaceuticals and in comparison with CT/MRI for the localization of sporadic metastatic pheochromocytoma and paraganglioma. Eur J Nucl Med Mol Imaging 2016;43:1784-91.
7. Jha A, Ling A, Millo C, Gupta G, Viana B, Lin FI, Herscovitch P, Adams KT, Taïeb D, Metwalli AR, Linehan WM, Brofferio A, Stratakis CA, Kebebew E, Lodish M, Civelek AC, Pacak K. Superiority of 68Ga-DOTATATE over 18F-FDG and anatomic imaging in the detection of succinate dehydrogenase mutation (SDHx)-related pheochromocytoma and paraganglioma in the pediatric population. Eur J Nucl Med Mol Imaging 2018;45:787-97.
8. Han S, Suh CH, Woo S, Kim YJ, Lee JJ. Performance of 68Ga-DOTA-Conjugated Somatostatin Receptor-Targeting Peptide PET in Detection of Pheochromocytoma and Paraganglioma: A Systematic Review and Metaanalysis. J Nucl Med 2019;60:369-76.
9. Janssen I, Chen CC, Taieb D, Patronas NJ, Millo CM, Adams KT, Nambuba J, Herscovitch P, Sadowski SM, Fojo AT, Buchmann I, Kebebew E, Pacak K. 68Ga-DOTATATE PET/CT in the Localization of Head and Neck Paragangliomas Compared with Other Functional Imaging Modalities and CT/MRI. J Nucl Med 2016;57:186-91.
10. Sharma P, Dhull VS, Arora S, Gupta P, Kumar R, Durgapal P, Malhotra A, Chumber S, Ammini AC, Kumar R, Bal C. Diagnostic accuracy of (68)Ga-DOTANOC PET/CT imaging in pheochromocytoma. Eur J Nucl Med Mol Imaging 2014;41:494-504.
11. Gild ML, Naik N, Hoang J, Hsiao E, McGrath RT, Sywak M, Sidhu S, Delbridge LW, Robinson BG, Schembri G, Clifton-Bligh RJ. Role of DOTATATE-PET/CT in preoperative assessment of phaeochromocytoma and

paragangliomas. Clin Endocrinol (Oxf) 2018;89:139-47.
12. Därr R, Kuhn M, Bode C, Bornstein SR, Pacak K, Lenders JWM, Eisenhofer G. Accuracy of recommended sampling and assay methods for the determination of plasma-free and urinary fractionated metanephrines in the diagnosis of pheochromocytoma and paraganglioma: a systematic review. Endocrine 2017;56:495-503.
13. Bozkurt MF, Virgolini I, Balogova S, Beheshti M, Rubello D, Decristoforo C, Ambrosini V, Kjaer A, Delgado-Bolton R, Kunikowska J, Oyen WJG, Chiti A, Giammarile F, Sundin A, Fanti S. Guideline for PET/CT imaging of neuroendocrine neoplasms with 68Ga-DOTA-conjugated somatostatin receptor targeting peptides and 18F-DOPA. Eur J Nucl Med Mol Imaging 2017;44:1588-601.
14. Taïeb D, Hicks RJ, Hindié E, Guillet BA, Avram A, Ghedini P, Timmers HJ, Scott AT, Elojeimy S, Rubello D, Virgolini IJ, Fanti S, Balogova S, Pandit-Taskar N, Pacak K. European Association of Nuclear Medicine Practice Guideline/Society of Nuclear Medicine and Molecular Imaging Procedure Standard 2019 for radionuclide imaging of phaeochromocytoma and paraganglioma. Eur J Nucl Med Mol Imaging 2019;46:2112-37.
15. Werner RA, Solnes LB, Javadi MS, Weich A, Gorin MA, Pienta KJ, Higuchi T, Buck AK, Pomper MG, Rowe SP, Lapa C. SSTR-RADS Version 1.0 as a Reporting System for SSTR PET Imaging and Selection of Potential PRRT Candidates: A Proposed Standardization Framework. J Nucl Med 2018;59:1085-91.
16. Elston MS, Meyer-Rochow GY, Conaglen HM, Clarkson A, Clifton-Bligh RJ, Conaglen JV, Gill AJ. Increased SSTR2A and SSTR3 expression in succinate dehydrogenase-deficient pheochromocytomas and paragangliomas. Hum Pathol 2015;46:390-6.
17. Nastos K, Cheung VTF, Toumpanakis C, Navalkissoor S, Quigley AM, Caplin M, Khoo B. Peptide Receptor Radionuclide Treatment and (131)I-MIBG in the management of patients with metastatic/progressive phaeochromocytomas and paragangliomas. J Surg Oncol 2017;115:425-34.
18. Unger N, Serdiuk I, Sheu SY, Walz MK, Schulz S, Saeger W, Schmid KW, Mann K, Petersenn S. Immunohistochemical localization of somatostatin receptor subtypes in benign and malignant adrenal tumours. Clin Endocrinol (Oxf) 2008;68:850-7.
19. Lenders JW, Pacak K, Walther MM, Linehan WM, Mannelli M, Friberg P, Keiser HR, Goldstein DS, Eisenhofer G. Biochemical diagnosis of pheochromocytoma: which test is best? JAMA 2002;287:1427-34.
20. Eisenhofer G, Goldstein DS, Walther MM, Friberg P, Lenders JW, Keiser HR, Pacak K. Biochemical diagnosis of pheochromocytoma: how to distinguish true- from false-positive test results. J Clin Endocrinol Metab 2003;88:2656-66.
21. Dietz M, Neyrand S, Dhomps A, Decaussin-Petrucci M, Tordo J. 18F-FDG PET/CT of a Rare Case of an Adenomatoid Tumor of the Adrenal Gland. Clin Nucl Med 2020;45:e331-3.
22. Guan J, Zhao C, Li H, Zhang W, Lin W, Tang L, Chen J. Adenomatoid Tumor of the Adrenal Gland: Report of Two Cases and Review of the Literature. Front Endocrinol (Lausanne) 2021;12:692553.

Cite this article as: Ma G, Du J, Zhang X, Liu J, Xu X, Xu B, Guan Z. Quantitative analysis of ^{68}Ga-DOTA(0)-Tyr(3)-octreotate positron emission tomography/computed tomography imaging for the differential diagnosis of primary pheochromocytoma and paraganglioma. Quant Imaging Med Surg 2022;12(4):2427-2440. doi: 10.21037/qims-21-652

